Report

Current Biology

Trans-endocytosis of Planar Cell Polarity Complexes during Cell Division

Highlights

- During mitosis, intercellular planar cell polarity complexes are trans-endocytosed
- Trans-internalized Celsr1 carries Fz6 and Vangl2 from neighboring cells
- Vangl2 proteins intrinsic to the dividing cell are retained on the surface
- Persistent Vangl2 stabilizes Celsr1 and delays its internalization

Authors

Bryan W. Heck, Danelle Devenport

Correspondence

danelle@princeton.edu

In Brief

During cell division, planar cell polarity (PCP) proteins are removed from the cell surface via bulk endocytosis. Heck and Devenport show that during this process, intercellular PCP complexes remain associated and are trans-endocytosed into dividing cells. Vangl2, however, is retained at the membrane, where it may act as a cue to restore polarity.

Heck & Devenport, 2017, Current Biology *27*, 3725–3733
December 4, 2017
https://doi.org/10.1016/j.cub.2017.10.053

CellPress

Current Biology
Report

Trans-endocytosis of Planar Cell Polarity Complexes during Cell Division

Bryan W. Heck[1] and Danelle Devenport[1,2,*]
[1]Department of Molecular Biology, Princeton University, 119 Lewis Thomas Laboratory, Washington Road, Princeton, NJ 08544, USA
[2]Lead Contact
*Correspondence: danelle@princeton.edu
https://doi.org/10.1016/j.cub.2017.10.053

SUMMARY

To coordinate epithelial architecture with proliferation, cell polarity proteins undergo extensive remodeling during cell division [1–3]. A dramatic example of polarity remodeling occurs in proliferative basal cells of mammalian epidermis whereupon cell division, transmembrane planar cell polarity (PCP) proteins are removed from the cell surface via bulk endocytosis [4]. PCP proteins form intercellular complexes, linked by Celsr1-mediated homophilic adhesion, that coordinate polarity non-autonomously between cells [5, 6]. Thus, the mitotic reorganization of PCP proteins must alter not only proteins intrinsic to the dividing cell but also their interacting partners on neighboring cells. Here, we show that intercellular Celsr1 complexes that connect dividing cells with their neighbors remain intact during mitotic internalization, resulting in an uptake of Celsr1 protein from interphase neighbors. Trans-internalized Celsr1 carries with it additional core PCP proteins, including the posteriorly enriched Fz6 and anteriorly enriched Vangl2. Cadherin-mediated homophilic adhesion is necessary for trans-endocytosis, and adhesive junctional PCP complexes appear to be destined for degradation upon internalization. Surprisingly, whereas Fz6 and Vangl2 both internalize in *trans*, Vangl2 proteins intrinsic to the dividing cell remain associated with the plasma membrane. Persistent Vangl2 stabilizes Celsr1 and impedes its internalization, suggesting that dissociation of Vangl2 from Celsr1 is a prerequisite for Celsr1 endocytosis. These results demonstrate an unexpected transfer of PCP complexes between neighbors and suggest that the Vangl2 population that persists at the membrane during cell division could serve as an internal cue for establishing PCP in new daughter cells.

RESULTS

Intercellular Celsr1 Complexes Undergo Trans-endocytosis into Dividing Cells

Core planar cell polarity (PCP) proteins form asymmetric, intercellular complexes at cell junctions where, on one side of an interface, transmembrane components Frizzled (Fz) and Flamingo (Fmi; Celsr in vertebrates) interact with Van Gogh (Vang; Vangl in vertebrates) and Fmi/Celsr on the neighboring cell via Fmi/Celsr-mediated homophilic adhesion (Figure 1A) [5, 7–14]. When basal cells of the mammalian epidermis divide, these transmembrane PCP proteins are removed from the cell surface and held within endosomes for the duration of mitosis, whereupon cytokinesis, they re-accumulate at the surface, and polarity is restored [4]. To address whether PCP bridges disassemble during mitotic internalization, we used genetic mosaics and cell mixing experiments to follow the origins and fates of PCP components in dividing cells and their immediate neighbors. First, we investigated the fate of junctional Celsr1 complexes by live imaging fluorescently labeled Celsr1 proteins in cultured epithelial cells. When keratinocytes expressing either Celsr1-mNeonGreen (Celsr1-Green) or Celsr1-mTagRFP-T (Celsr1-Red) were mixed and grown as an epithelial monolayer, the endosomes of dividing cells contained both green and red Celsr1, indicating that dividing cells had internalized not only their own Celsr1 protein but also that of their neighbors (Figure 1B). Since both fluorescent proteins were fused to the C-terminal cytosolic domain, Celsr1 entered the mitotic cell in its full-length form and not after being cleaved extracellularly. We refer to the internalization of junctional Celsr1 homodimers as trans-endocytosis.

In basal cells of the embryonic epidermis, Celsr1 localizes asymmetrically to anterior and posterior cell junctions, but at the interfaces between mitotic cells and their neighbors, Celsr1 was largely absent (Figures 1A and 1C) [15]. To test directly whether trans-endocytosis of Celsr1 can account for this observation *in vivo*, we utilized transgenic mouse embryos expressing Celsr1-GFP in a mosaic pattern [4], allowing us to distinguish Celsr1 molecules intrinsic to the dividing cell from those of its neighbors. In dividing cells located along the boundaries of Celsr1-GFP expression, GFP-positive puncta were observed in the cytoplasm, suggesting that they had derived from neighboring Celsr1-GFP-positive cells (Figure 1D). This was confirmed using a second transgenic line expressing bicistronic Celsr1-GFP and H2B-RFP separated by a 2A cleavage site. Mitotic cells that lacked nuclear H2B-RFP, and hence Celsr1-GFP expression, contained GFP-positive puncta in the vicinity of H2B-RFP-positive neighbors (Figure 1E). Thus, intercellular Celsr1 complexes remain associated during mitotic endocytosis and are co-internalized, leaving the adhesive interface between the dividing cell and its neighbors largely devoid of Celsr1 protein.

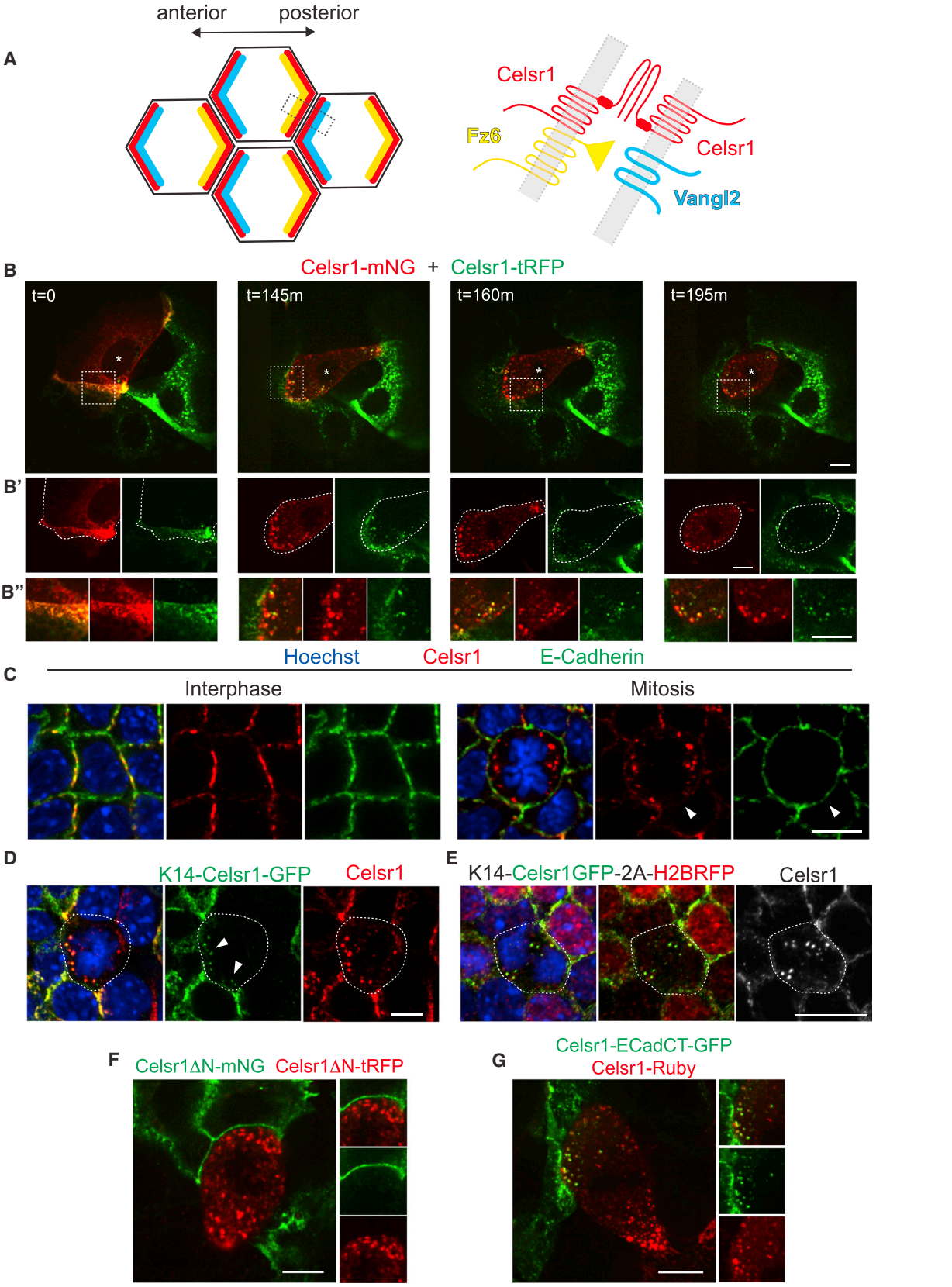

(legend on next page)

Celsr1 Domains Required for Trans-endocytosis

Celsr1's extracellular domain mediates calcium-dependent adhesion, whereas sequences within the intracellular domain control mitotic internalization [4, 15, 16]. To determine whether trans-endocytosis requires Celsr1's homophilic adhesive interactions, we performed a cell mixing experiment with a truncated form of Celsr1 lacking most of the extracellular domain (Celsr1-ΔN). As expected, adhesion-deficient Celsr1-ΔN was internalized during mitosis, but mitotic endosomes contained only Celsr1-ΔN from the dividing cell and not from its neighbors (Figure 1F). To test whether Celsr1's intracellular domain, which is necessary and sufficient for internalization in *cis*, is needed in the neighboring cell for trans-internalization, we replaced Celsr1's cytosolic tail with the intracellular domain of E-Cadherin. When interphase cells expressing the Celsr1-ECadCT chimera were juxtaposed to dividing cells expressing wild-type Celsr1, the chimeric protein was trans-endocytosed into mitotic endosomes (Figure 1G). Thus, Celsr1 trans-endocytosis requires a cytoplasmic internalization signal only within the dividing cell plus an extracellular interaction to pull in Celsr1 proteins from the neighbor.

Fate of Celsr1 Trans-endosomes following Internalization

Trans-endocytosis of Celsr1 homodimers is predicted to generate a double-membrane vesicle, an architecture that seems incompatible with recycling to the plasma membrane. To decipher the fate of Celsr1 trans-endosomes following internalization, we performed a pulse-chase experiment using a green-to-red photoswitchable fluorophore fused to Celsr1 (Celsr1-mEos3.2), allowing us to unambiguously label the trans-endocytosed pool of Celsr1. In this experiment, Celsr1-mEos3.2 that had trans-internalized into a dividing cell (expressing Celsr1-Blue) was locally photoswitched from green to red and followed by time-lapse imaging through cytokinesis. Instead of accumulating at the plasma membrane, red fluorescence progressively decreased over time, suggesting that trans-endocytosed Celsr1-mEos3.2 proteins were being lost to degradation (Figures S1A and S1C). The loss of endosomal fluorescence was not due to photobleaching, as photoswitched Celsr1-mEos3.2 at a neighboring interphase junction was stable over the same period (Figures S1A and S1C). *cis*-internalizalized Celsr1-mEos3.2 was also lost over time (Figures S1B and S1C), suggesting that endosomes containing Celsr1 molecules engaged in intercellular adhesion cannot be recycled to the cell surface. Trans-endosomes colocalized with the late endosomal marker Rab7, supporting the conclusion that trans-endosomes are transported to lysosomes for degradation (Figure S1D).

To monitor the fate of adhesion-deficient Celsr1 molecules, which are presumed to internalize into single-membrane vesicles and recycle, we fused an extracellular hemagglutinin (HA) epitope tag to Celsr1-ΔN-GFP, allowing us to selectively label the surface pool of Celsr1-ΔN and follow internalized proteins through cytokinesis. Time-lapse imaging and pulse-chase assays demonstrated that, although internalized HA-Celsr1-ΔN-GFP was capable of recycling to the surface (Figures S2B and S2C), a significant proportion of internalized Celsr1-ΔN failed to recycle and accumulated around the nuclei of new daughter cells (Figure S2A). In addition, unlabeled, newly synthesized proteins contributed significantly to Celsr1-ΔN surface localization following division (Figure S2A). Together, these findings imply that the reestablishment of planar polarity following division depends primarily on newly synthesized PCP proteins.

Frizzled-6 Undergoes Both *cis* and Trans-endocytosis

To determine whether mitotic cells internalize other PCP proteins from their neighbors, we performed a cell mixing assay where cells co-expressing Fz6-Red and Celsr1-Blue were intermingled with cells expressing Celsr1-Green alone (see figure legends for specific fluorophores). When Fz6-Red was expressed in the interphase neighbor, Celsr1-Green mitotic endosomes also contained red fluorescent protein, indicating that Fz6 had been trans-endocytosed from the neighboring cell (Figure 2A). Fz6-Red was also drawn into mitotic endosomes when it was co-expressed with adhesion-deficient Celsr1-ΔN (Figure 2B), indicating that, like Celsr1, Fz6 molecules undergo both *cis* and trans-endocytosis.

Next, we sought to determine the origins of internalized Fz6 *in vivo*. In interphase cells, Fz6 co-localizes with Celsr1 at cell junctions [15] and, by extension with what is known in *Drosophila*, preferentially to the posterior side. However, in dividing cells, Fz6-containing endosomes were found on both sides of the cell, suggesting that Fz6 was being internalized from both the dividing cell and its neighbor. To quantify the distribution of endogenous Fz6, we compared the correlation coefficients of Celsr1 and Fz6 on the anterior and posterior halves of dividing

Figure 1. Celsr1 Is Trans-endocytosed into Dividing Cells

(A) Schematic representation of PCP protein localization.

(B) Time-lapse images of cell mixing assay with a Celsr1-mNeonGreen (mNG; shown in red) cell adhering to two Celsr1-mTagRFP-T (tRFP; shown in green) cells. Prior to division (t = 0), Celsr1-mNG and Celsr1-tRFP colocalize at cell interfaces (yellow in B, channels separated in B', and magnified in B''). Upon mitosis (t = 145 min), Celsr1-tRFP from the neighboring interphase cell is drawn into the mitotic Celsr1-mNG cell. Pearson's correlation coefficient r = 0.78. Asterisks mark the dividing cell. See also Figure S1 for the fate of Celsr1 trans-endosomes following mitosis.

(C) E15.5 whole-mount epidermis immunolabeled with Celsr1 (red) and E-Cadherin (green) antibodies. In mitosis (right), little Celsr1 remains on the cell surface.

(D) E15.5 transgenic embryo mosaically expressing Celsr1-GFP (K14-Celsr1-GFP). Shown is a GFP- basal cell in mitosis (outlined) adjacent to GFP+ (green) cluster. GFP+ puncta colocalize with endogenous Celsr1 (red).

(E) E15.5 transgenic embryo mosaically expressing Celsr1-GFP-2A-H2B-RFP. A basal cell in mitosis (outlined) lacking H2B-RFP surrounded by Celsr1-GFP-2A-H2B-RFP-expressing cells contains GFP+ puncta (green) that colocalize with endogenous Celsr1 (grayscale).

(F) Cell mixing assay between cells expressing adhesion-deficient Celsr1-ΔN-mNG or Celsr1-ΔN-TagRFP (tRFP). Celsr1-ΔN-mNG (green) from the interphase neighbor remains on the surface. See also Figure S2 for the fate of adhesion-deficient Celsr1-ΔN in cytokinesis.

(G) Cell mixing assay between cells expressing Celsr1-ECadCT-GFP or Celsr1-mRuby3 (red). The chimeric protein (green) containing the intracellular domain of E-Cadherin, is trans-internalized.

Pearson's r = 0.73. Scale bars, 10 μm. Anterior is left.

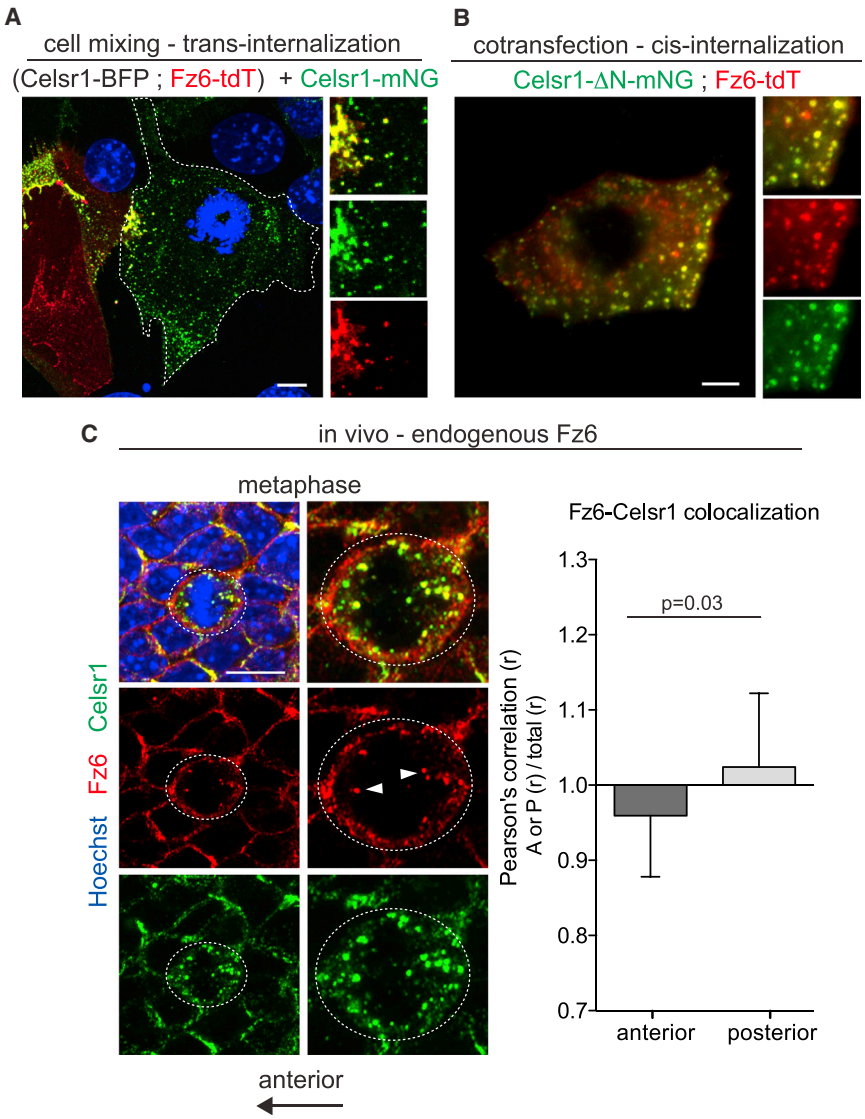

Figure 2. Frizzled-6 Is Internalized in Both *cis* and *trans*

(A) Cell mixing assay with keratinocytes expressing Celsr1-mNG alone (green) or Celsr1-mTagBFP2 (BFP) + Fz6-tdTomato (tdT, red). Fz6-tdT from the interphase neighbor trans-internalizes into the Celsr1-mNG dividing cell; Pearson's r = 0.77.

(B) Keratinocytes co-expressing adhesion-deficient Celsr1-ΔN-mNG (green) and Fz6-tdT (red). Celsr1-ΔN-mNG is sufficient to co-internalize Fz6-tdT; Pearson's r = 0.78.

(C) Confocal section of whole-mount E15.5 epidermis immunolabeled with Fz6 (red) and Celsr1 (green) antibodies. Fz6 puncta are located on both sides of the dividing cell (arrowheads). Colocalization between Fz6 and Celsr1 on the anterior and posterior halves of the cell is represented by the Pearson's correlation coefficient (*r*) relative to the *r* value of the total cell. n = 20. Mean + SD are shown. p = 0.028, unpaired t test. Scale bars, 10 μm. Anterior is left.

cells and found that they were roughly equivalent, even though Fz6 is thought to reside primarily on the posterior side (Figure 2C). These results are consistent with the idea that on the posterior side, Fz6 is internalized from the mitotic cell surface and on the anterior side, Fz6 is taken up from the neighboring interface.

During Mitosis, Vangl2 Is Internalized Predominantly in *trans*

Vangl2 was also previously observed to localize to mitotic endosomes [4], so we sought to determine whether internalized Vangl2 proteins derive from the mitotic cell and/or their neighbors. As before, a cell mixing assay was used to test whether Vangl2 could be internalized in *trans*, where Celsr1-Green cells were intermingled with cells co-expressing Celsr1-Blue and Vangl2-Red. When a Vangl2-Red-expressing cell was juxtaposed to Celsr1-Green cell in mitosis, Vangl2-Red was trans-internalized along with Celsr1 into the dividing cell (Figure 3A). Unexpectedly, when Vangl2 was expressed from within the dividing cell itself, it was not internalized in *cis* (Figure 3B). Instead, Vangl2 remained at the cell surface, where it appeared to sequester a fraction of Celsr1-ΔN-GFP to the plasma membrane (Figure 3B). Together, these *in vitro* experiments suggest that, while Celsr1 can internalize Vangl2 from neighboring cells, it cannot co-internalize Vangl2 proteins from within the dividing cell itself.

To determine the source of internalized Vangl2 *in vivo*, we examined the localization of mitotic PCP endosomes in transgenic embryos that express mosaic GFP-Vangl2. In interphase cells, GFP-Vangl2 localizes to the anterior side of intercellular junctions (Figure 3C, top panels) [4], but in dividing cells, GFP-Vangl2-containing endosomes were positioned oppositely on the posterior side, suggesting that they had derived from the anterior surface of the neighboring cell. Indeed, when a patch of GFP-Vangl2-expressing cells bordered a cell in mitosis on its posterior, the dividing cell contained posterior GFP+ endosomes, even when it lacked transgene expression (Figure 3C, middle panels; Figure S3A). By contrast, dividing cells that expressed GFP-Vangl2 lacked GFP+ endosomes on their anterior sides and retained Vangl2 proteins intrinsic to the dividing cell on the cell surface (Figure 3C, bottom panels; Figure S3B). These results were corroborated by examining the distribution of endogenous Vangl2 in dividing cells *in vivo*, where the average colocalization between Celsr1 and Vangl2 was significantly greater on the posterior side than on the anterior side (Figure 3D). Interestingly, this posterior bias was observed even during cytokinesis, suggesting that the mobility of PCP-containing endosomes is fairly limited (Figure 3D).

Collectively, our results are summarized in Figure 3E and suggest that PCP components are internalized into dividing cells as intercellular complexes. Dividing cells contain at least two

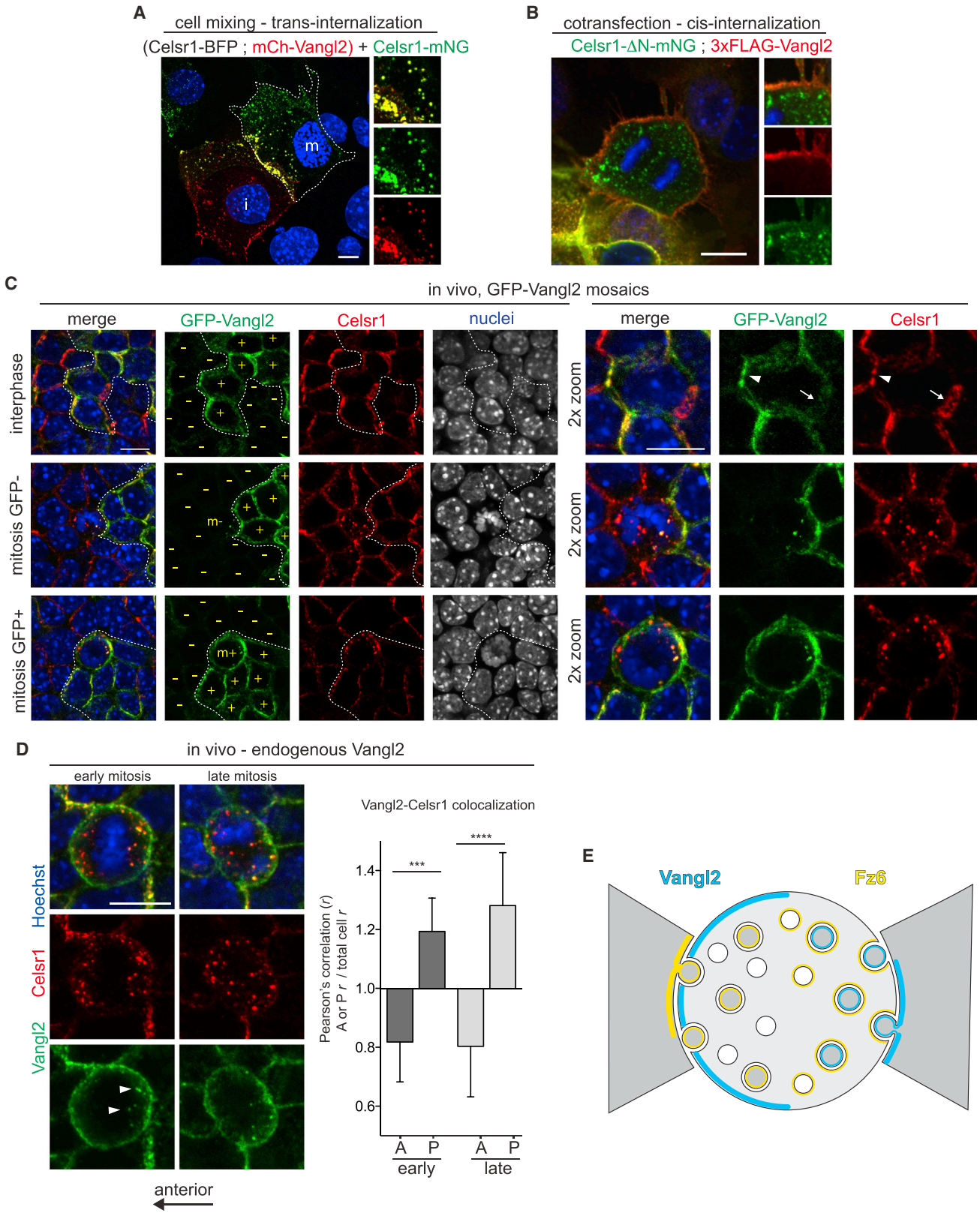

(legend on next page)

distinct pools of trans-endosomes with polarized distributions: one that is anteriorly localized and contains Fz6 from the neighboring cells but lacks Vangl2 and another posteriorly localized pool that contains the full complement of transmembrane PCP components derived from both the mitotic and neighboring cell membranes. Trans-endocytosis removes a significant proportion of PCP proteins from neighboring cell interfaces, which appear to be destined for degradation, while leaving Vangl2 behind on the surface of the dividing cell.

Vangl2 Stabilizes Celsr1 at the Cell Surface

In non-dividing cells of the *Drosophila* wing, Vang serves to stabilize Fmi at intercellular junctions by protecting Fmi from endocytosis [17]. The unexpected separation of Vangl2 from Celsr1 during cell division suggested that Vangl2 might also have a stabilizing effect in basal cells and thus need to be physically uncoupled from Celsr1 to allow efficient mitotic internalization. Indeed, we noted that on the anterior side of dividing cells where Vangl2 protein persists at the surface, Celsr1 internalization was delayed. By prometaphase, posterior Celsr1 had internalized, whereas anterior Celsr1 was frequently retained on the surface until metaphase (Figure 4A). This delay was not observed in embryos lacking epidermal Vangl1 and Vangl2 (Figure 4B), but in embryos lacking Fz6, where Vangl2 localizes more uniformly at the cell cortex (Figure S4), Celsr1 persisted at the membrane through metaphase (Figures 4C and 4D). Overexpression of Vangl2 also caused a significant fraction of Celsr1-ΔN to be retained at the cell surface in dividing keratinocytes (Figure 4E), which we analyzed quantitatively using surface labeling of extracellular HA-tagged Celsr1-ΔN-GFP. When Vangl2 was overexpressed with HA-Celsr1-ΔN-GFP, Celsr1 surface levels were increased and comparable to their interphase levels, whereas overexpression with Fz6 had no effect (Figures 4F and 4G). Thus, Vangl2 protects Celsr1 from being endocytosed and delays internalization on the anterior side, suggesting that the two proteins must be actively uncoupled to allow for Celsr1 internalization.

DISCUSSION

Here, we demonstrate that, when epidermal basal cells divide, junctional PCP proteins are endocytosed into dividing cells as intercellular complexes, where trans-internalized Celsr1 carries Fz6 and Vangl2 from neighboring cells. Together with other known examples of trans-endocytosis, including Notch-Delta, Eph-ephrin, the connexin subunits of gap junctions, and MHC-T cell receptor complexes [18–24], our findings highlight a pervasive intercellular exchange of transmembrane proteins between cells and suggest that trans-endocytosis may be rather widespread. Celsr1 internalization bears a similarity to gap junction turnover, where large, double-membrane vesicles known as "annular junctions" internalize entire gap junction plaques that go on to be degraded [22, 25].

Whether trans-endocytosis is simply the outcome of highly avidity intercellular interactions between PCP proteins or whether it serves a specific function in PCP remains unclear. In fact, the specific function served by mitotic internalization remains mysterious [4, 16]. We proposed that internalization could ensure that PCP proteins are equally inherited into daughter cells, but the posterior localization of Vangl2-containing endosomes and evidence that trans-endocytosed PCP proteins are probably degraded suggest that new PCP protein synthesis is what equilibrates PCP surface levels during cytokinesis. Given the apparent high avidity binding of Celsr1 homodimers, and their relatively slow mobility and turnover [26], perhaps endocytic removal of Celsr1 allows cells to more readily remodel cell junctions and to quickly reposition PCP proteins after mitotic cell rearrangements. To restore polarity following cytokinesis, we proposed that dividing cells use PCP cues from their neighbors [4]. However, our present data show that trans-endocytosis removes most, if not all, Celsr1 from the neighboring interface and raise the intriguing possibility that Vangl2 proteins retained at the membrane could serve as an internal, cell-autonomous memory of planar polarity.

Finally, we provide evidence that anterior Vangl2 stabilizes and protects Celsr1 from internalization, which is in line with reports in *Drosophila* that Vang increases junctional Fmi and prevents its endocytic turnover [11, 17]. It is unclear whether anterior Celsr1 retention serves a function during cell division or whether it simply reflects the time required for Celsr1 to be physically uncoupled from Vangl2 upon mitotic entry. The mitotic kinase Plk1 initiates Celsr1 internalization via phosphorylation, which could similarly trigger Vangl2 and Celsr1 dissociation [16]. Defining the function of retained Vangl2 and the mechanism that uncouples it from Celsr1 will be important future avenues to explore.

STAR★METHODS

Detailed methods are provided in the online version of this paper and include the following:

- KEY RESOURCES TABLE
- CONTACT FOR REAGENT AND RESOURCE SHARING

Figure 3. Vangl2 Is Internalized Predominantly in *trans*

(A) Cell mixing assay between keratinocytes expressing Celsr1-mNG (green) alone and Celsr1-BFP + mCh-Vangl2 (red). Endosomes of the Celsr1-mNG mitotic cell (m, outlined) contain mCh-Vangl2 derived from the interphase neighbor (i). Pearson's r = 0.83.

(B) Keratinocytes co-expressing Celsr1-ΔN-mNG (green) and 3xFLAG-Vangl2 (red). Celsr1-ΔN-mNG does not co-internalize 3xFLAG-Vangl2. Pearson's r = 0.27.

(C) E15.5 transgenic embryonic epidermis mosaically expressing GFP-Vangl2 (green). Left panels show regions of mosaic expression at low magnification. Right panels show borders of mosaicism at 2× zoom. Dotted lines mark borders of GFP-Vangl2 expression, and individual cells are marked as either + or − for GFP. Top row: GFP-Vangl2 in interphase is enriched on anterior cell borders. Middle row: a GFP-negative cell in mitosis (m-) adjacent to GFP-Vangl2-expressing cells contains posterior GFP+ puncta that colocalize with endogenous Celsr1 (red). Bottom row: GFP-Vangl2-expressing cell in mitosis (m+) lacks GFP+ puncta on the anterior side. See also Figure S3 for additional examples.

(D) Basal cells in metaphase and anaphase from E15.5 dorsal skin immunolabeled with Vangl2 (green) and Celsr1 (red) antibodies showing posterior Vangl2 puncta. Colocalization between Vangl2 and Celsr1 on the anterior and posterior halves of the cell is represented by the Pearson's correlation coefficient (r) normalized to the *r* value of the total cell. n = 11 cells, early mitosis; n = 15 cells, late mitosis; mean + SD are shown. ***p < 0.001, ****p < 0.0001, unpaired t test.

(E) Schematic representation of mitotic trans-endocytosis.

Scale bars, 10 μm. Anterior is left.

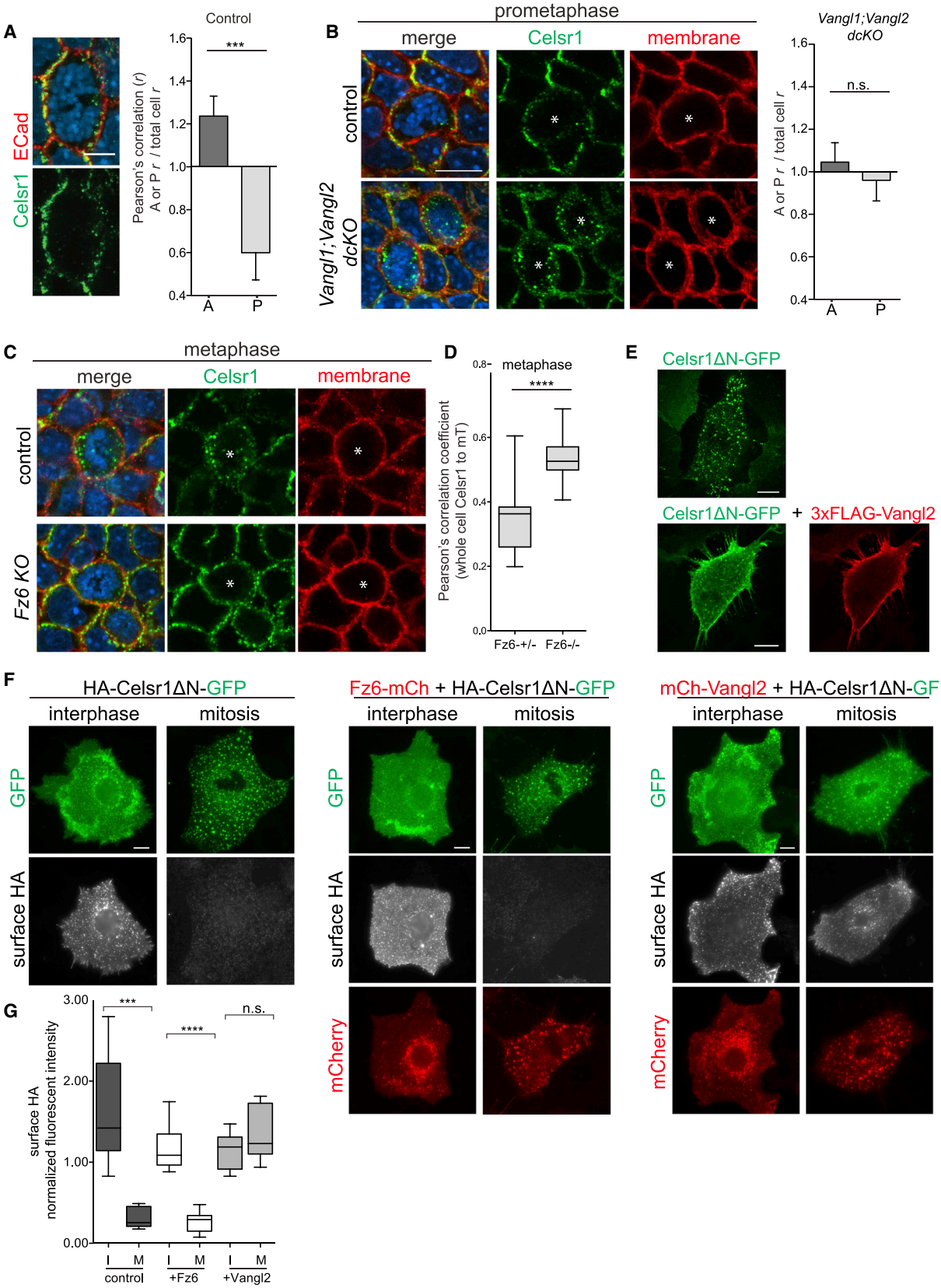

(legend on next page)

- EXPERIMENTAL MODEL AND SUBJECT DETAILS
  - Mice
  - Cell lines
- METHOD DETAILS
  - Molecular cloning and constructs
  - Cell mixing assays
  - Photoconversion assay
  - Celsr1 surface labeling
  - Celsr1 recycling assay
  - Immunostaining and image acquisition
- QUANTIFICATION AND STATISTICAL ANALYSIS
  - Quantification of vesicle enrichment
  - Quantification of Celsr1 surface labeling
  - Quantification of Vangl2 asymmetry
  - Statistical Analysis

SUPPLEMENTAL INFORMATION

Supplemental Information includes four figures and can be found with this article online at https://doi.org/10.1016/j.cub.2017.10.053.

AUTHOR CONTRIBUTIONS

B.W.H. designed and performed experiments and data analysis. D.D. oversaw experimental design and data analysis, performed experiments, and wrote the manuscript.

ACKNOWLEDGMENTS

We thank Katie Little, Maureen Cetera, and Liliya Leybova for technical assistance; Gary Laevsky, and the Nikon Center for Excellence confocal core facility for imaging expertise; the CINJ Genome Editing Facility for transgenic mice; and Jean-Paul Borg, who provided the Vangl2 antibody. We thank Eric Wieschaus and Elizabeth Gavis for insightful discussion and feedback on the manuscript. Research reported in this publication was supported by the National Institute of Arthritis and Musculoskeletal and Skin Diseases of the NIH under award number R01AR068320. This material is based upon work supported by the National Science Foundation Graduate Research Fellowship under grant no. DGE-1656466.

Received: May 27, 2017
Revised: September 15, 2017
Accepted: October 19, 2017
Published: November 22, 2017

REFERENCES

1. Ragkousi, K., and Gibson, M.C. (2014). Cell division and the maintenance of epithelial order. J. Cell Biol. *207*, 181–188.
2. Macara, I.G., Guyer, R., Richardson, G., Huo, Y., and Ahmed, S.M. (2014). Epithelial homeostasis. Curr. Biol. *24*, R815–R825.
3. Morin, X., and Bellaïche, Y. (2011). Mitotic spindle orientation in asymmetric and symmetric cell divisions during animal development. Dev. Cell *21*, 102–119.
4. Devenport, D., Oristian, D., Heller, E., and Fuchs, E. (2011). Mitotic internalization of planar cell polarity proteins preserves tissue polarity. Nat. Cell Biol. *13*, 893–902.
5. Butler, M.T., and Wallingford, J.B. (2017). Planar cell polarity in development and disease. Nat. Rev. Mol. Cell Biol. *18*, 375–388.
6. Devenport, D. (2014). The cell biology of planar cell polarity. J. Cell Biol. *207*, 171–179.
7. Yang, Y., and Mlodzik, M. (2015). Wnt-Frizzled/planar cell polarity signaling: cellular orientation by facing the wind (Wnt). Annu. Rev. Cell Dev. Biol. *31*, 623–646.
8. Goodrich, L.V., and Strutt, D. (2011). Principles of planar polarity in animal development. Development *138*, 1877–1892.
9. Usui, T., Shima, Y., Shimada, Y., Hirano, S., Burgess, R.W., Schwarz, T.L., Takeichi, M., and Uemura, T. (1999). Flamingo, a seven-pass transmembrane cadherin, regulates planar cell polarity under the control of Frizzled. Cell *98*, 585–595.
10. Chen, W.S., Antic, D., Matis, M., Logan, C.Y., Povelones, M., Anderson, G.A., Nusse, R., and Axelrod, J.D. (2008). Asymmetric homotypic interactions of the atypical cadherin flamingo mediate intercellular polarity signaling. Cell *133*, 1093–1105.
11. Strutt, H., and Strutt, D. (2008). Differential stability of flamingo protein complexes underlies the establishment of planar polarity. Curr. Biol. *18*, 1555–1564.
12. Wu, J., and Mlodzik, M. (2008). The frizzled extracellular domain is a ligand for Van Gogh/Stbm during nonautonomous planar cell polarity signaling. Dev. Cell *15*, 462–469.
13. Lawrence, P.A., Casal, J., and Struhl, G. (2004). Cell interactions and planar polarity in the abdominal epidermis of *Drosophila*. Development *131*, 4651–4664.
14. Struhl, G., Casal, J., and Lawrence, P.A. (2012). Dissecting the molecular bridges that mediate the function of Frizzled in planar cell polarity. Development *139*, 3665–3674.
15. Devenport, D., and Fuchs, E. (2008). Planar polarization in embryonic epidermis orchestrates global asymmetric morphogenesis of hair follicles. Nat. Cell Biol. *10*, 1257–1268.
16. Shrestha, R., Little, K.A., Tamayo, J.V., Li, W., Perlman, D.H., and Devenport, D. (2015). Mitotic control of planar cell polarity by Polo-like Kinase 1. Dev. Cell *33*, 522–534.
17. Strutt, H., Warrington, S.J., and Strutt, D. (2011). Dynamics of core planar polarity protein turnover and stable assembly into discrete membrane subdomains. Dev. Cell *20*, 511–525.
18. Klueg, K.M., and Muskavitch, M.A. (1999). Ligand-receptor interactions and trans-endocytosis of Delta, Serrate and Notch: members of the Notch signalling pathway in *Drosophila*. J. Cell Sci. *112*, 3289–3297.

Figure 4. Vangl2 Antagonizes Celsr1 Internalization

(A) Basal cell in prophase showing anterior retention of Celsr1 (green) (red, E-Cadherin; blue, Hoechst). Pearson's correlation coefficients (r) of Celsr1 and E-Cadherin at anterior and posterior halves of cells in prophase. Mean + SD are shown. p = 0.0002, unpaired t test.
(B) Control and *Vangl1;Vangl2 dcKO* basal cells in prometaphase (asterisks). Pearson's correlation coefficients (*r*) between Celsr1 (green) and membrane-GFP (red) at anterior and posterior halves of early mitotic cells. Mean + SD are shown. n = 10; p = 0.294, unpaired t test. n.s., not significant.
(C) Control and *Fz6 KO* basal cells in metaphase (asterisks) labeled with Celsr1 (green) and membrane-tdTomato (red).
(D) Whole-cell Pearson's correlation coefficient (*r*) between Celsr1 and membrane-tdTomato at metaphase was significantly increased in Fz6 KOs (knockouts): n = 15, heterozygous; n = 30, KO; p < 0.0001, unpaired t test. See also Figure S4 for Vangl2 localization in Fz6 KO.
(E) Dividing keratinocytes expressing Celsr1-ΔN-GFP alone (top) or with 3xFLAG-Vangl2 (bottom).
(F) Keratinocytes expressing HA-Celsr1-ΔN-GFP (green) alone or with mCherry-Vangl2 or Fz6-mCherry (red). Surface HA-Celsr1-ΔN was labeled with anti-HA antibody without permeablization (grayscale).
(G) Quantification of surface HA normalized to total GFP expression. HA-Celsr1-ΔN-GFP: n = 9, interphase; n = 10, mitosis; p = 0.0004. +Fz6-mCherry: n = 12, interphase; n = 12, mitosis; p < 0.0001. +mCherry-Vangl2: n = 10, interphase; n = 9, mitosis; p = 0.147, unpaired t test with Welch's correction.
***p < 0.001, ****p < 0.0001; n.s., not significant. Scale bars, 10 μm. Anterior is left.

19. Parks, A.L., Klueg, K.M., Stout, J.R., and Muskavitch, M.A. (2000). Ligand endocytosis drives receptor dissociation and activation in the Notch pathway. Development *127*, 1373–1385.

20. Marston, D.J., Dickinson, S., and Nobes, C.D. (2003). Rac-dependent trans-endocytosis of ephrinBs regulates Eph-ephrin contact repulsion. Nat. Cell Biol. *5*, 879–888.

21. Zimmer, M., Palmer, A., Köhler, J., and Klein, R. (2003). EphB-ephrinB bi-directional endocytosis terminates adhesion allowing contact mediated repulsion. Nat. Cell Biol. *5*, 869–878.

22. Falk, M.M., Bell, C.L., Kells Andrews, R.M., and Murray, S.A. (2016). Molecular mechanisms regulating formation, trafficking and processing of annular gap junctions. BMC Cell Biol. *17* (*Suppl 1*), 22.

23. Davis, D.M. (2007). Intercellular transfer of cell-surface proteins is common and can affect many stages of an immune response. Nat. Rev. Immunol. *7*, 238–243.

24. Rechavi, O., Goldstein, I., and Kloog, Y. (2009). Intercellular exchange of proteins: the immune cell habit of sharing. FEBS Lett. *583*, 1792–1799.

25. Thévenin, A.F., Kowal, T.J., Fong, J.T., Kells, R.M., Fisher, C.G., and Falk, M.M. (2013). Proteins and mechanisms regulating gap-junction assembly, internalization, and degradation. Physiology (Bethesda) *28*, 93–116.

26. Aw, W.Y., Heck, B.W., Joyce, B., and Devenport, D. (2016). Transient tissue-scale deformation coordinates alignment of planar cell polarity junctions in the mammalian skin. Curr. Biol. *26*, 2090–2100.

27. Belotti, E., Puvirajesinghe, T.M., Audebert, S., Baudelet, E., Camoin, L., Pierres, M., Lasvaux, L., Ferracci, G., Montcouquiol, M., and Borg, J.P. (2012). Molecular characterisation of endogenous Vangl2/Vangl1 heteromeric protein complexes. PLoS ONE *7*, e46213.

28. Chang, H., Smallwood, P.M., Williams, J., and Nathans, J. (2016). The spatio-temporal domains of Frizzled6 action in planar polarity control of hair follicle orientation. Dev. Biol. *409*, 181–193.

29. Copley, C.O., Duncan, J.S., Liu, C., Cheng, H., and Deans, M.R. (2013). Postnatal refinement of auditory hair cell planar polarity deficits occurs in the absence of Vangl2. J. Neurosci. *33*, 14001–14016.

30. Guo, N., Hawkins, C., and Nathans, J. (2004). Frizzled6 controls hair patterning in mice. Proc. Natl. Acad. Sci. USA *101*, 9277–9281.

31. Yusa, K., Zhou, L., Li, M.A., Bradley, A., and Craig, N.L. (2011). A hyperactive piggyBac transposase for mammalian applications. Proc. Natl. Acad. Sci. USA *108*, 1531–1536.

32. Aigouy, B., Farhadifar, R., Staple, D.B., Sagner, A., Röper, J.C., Jülicher, F., and Eaton, S. (2010). Cell flow reorients the axis of planar polarity in the wing epithelium of *Drosophila*. Cell *142*, 773–786.

33. Nowak, J.A., and Fuchs, E. (2009). Isolation and culture of epithelial stem cells. Methods Mol. Biol. *482*, 215–232.

STAR★METHODS

KEY RESOURCES TABLE

REAGENT or RESOURCE	SOURCE	IDENTIFIER
Antibodies		
Guinea pig polyclonal anti-Celsr1	D.D. and E. Fuchs [15]	N/A
Goat polyclonal anti-Fzd6	R&D Systems	Cat #AF1526
Rat monoclonal anti-Vangl2, clone 2G4	Jean-Paul Borg [27]; Millipore	Cat #MABN750
Rat monoclonal anti-E-Cadherin, clone DECMA-1	Thermo-Pierce	Cat #MA1-25160
Rabbit polyclonal anti-Rab7	Cell Signaling	Cat #D95F2
Mouse monoclonal anti-FLAG	Sigma	Cat #F1804
Rat monoclonal anti-HA	Roche	Cat #11867423001
647-conjugated mouse monoclonal anti-HA	Cell Signaling	Cat #3444
Chemicals, Peptides, and Recombinant Proteins		
CDK1 inhibitor RO-3306	Sigma	Cat #SML0569
Critical Commercial Assays		
Effectene Transfection reagent	QIAGEN	Cat. #301427
Experimental Models: Cell Lines		
pBacK14::Celsr1-mRuby3 (mouse CD1 keratinocytes)	This paper	N/A
pBacK14::Celsr1-mNeonGreen (mouse CD1 keratinocytes)	This paper	N/A
pBacK14::Celsr1-mEos3.2 (mouse CD1 keratinocytes)	This paper	N/A
pBacK14::Celsr1-mTagBFP2 (mouse CD1 keratinocytes)	This paper	N/A
pBacK14::Celsr1-mTagRFP-T (mouse CD1 keratinocytes)	This paper	N/A
K14retro::Celsr1ΔN-mNeonGreen (mouse CD1 keratinocytes)	This paper	N/A
K14retro::Celsr1ΔN-mTagRFP-T (mouse CD1 keratinocytes)	This paper	N/A
K14retro::3xFLAG-Vangl2 (mouse CD1 keratinocytes)	This paper	N/A
Experimental Models: Organisms/Strains		
CD-1 (*Mus musculus*)	Charles River	Strain #022
Tg(K14::GFP-Vangl2) (*Mus musculus*)	D.D. and E. Fuchs [4]	N/A
Tg(K14::Celsr1-GFP) (*Mus musculus*)	D.D. and E. Fuchs [4]	N/A
Tg(K14-Cre); Vangl1[fl/fl] ; Vangl2[fl/delTM] ; ROSA26[mTmG/+] (*Mus musculus*)	J. Nathans and M. Deans [28, 29]	N/A
Fz6 [tm1Nat/tm1Nat] ; ROSA26[mTmG/+] (*Mus musculus*)	J. Nathans [30], Jackson Labs	Stock #012824
K14::Celsr1-GFP-F2A-H2B-RFP (*Mus musculus*)	This paper	N/A
Recombinant DNA		
pBacK14-Celsr1-mNeonGreen	This paper	N/A
pBacK14-Celsr1-mRuby3	This paper	N/A
pBacK14-Celsr1-mEos3.2	This paper	N/A
pBacK14-Celsr1-mTagBFP2	This paper	N/A
pBacK14-Celsr1-mTagRFP-T	This paper	N/A
K14-Celsr1-ECadCT-GFP	This paper	N/A
K14retro-Celsr1ΔN-mNeonGreen	This paper	N/A

(*Continued on next page*)

Continued

REAGENT or RESOURCE	SOURCE	IDENTIFIER
K14retro-Celsr1ΔN-mTagRFP-T	This paper	N/A
K14retro-HA-Celsr1ΔN-GFP	This paper	N/A
K14-Frizzled6-tdTomato	This paper	N/A
K14-Fzd6-mCherry	D.D. and E. Fuchs [15]	N/A
K14-mCherry-Vangl2	D.D. and E. Fuchs [15]	N/A
K14retro-3xFLAG-Vangl2	This paper	N/A
mTagRFP-T	gift from Michael Davidson	Addgene #54586
mRuby3	gift from Michael Davidson	Addgene #74252
mTagBFP2	gift from Michael Davidson	Addgene #54602,
mEos3.2	gift from Michael Davidson	Addgene #54550
pCMV-hyPBase	Wellcome Trust Sanger Institute [31]	N/A
Software and Algorithms		
Colocalization Test	Fiji (ImageJ)	https://imagej.net/Colocalization_Test
Packing Analyzer V2	Benoit Aigouy [32]	https://idisk-srv1.mpi-cbg.de/~eaton/

CONTACT FOR REAGENT AND RESOURCE SHARING

Further information and requests for resources and reagents should be directed to and will be fulfilled by the Lead Contact, Danelle Devenport (danelle@princeton.edu).

EXPERIMENTAL MODEL AND SUBJECT DETAILS

Mice

Stage E15.5 embryos (male and female) were derived from the following lines: CD1, K14-GFP-Vangl2 [4]; K14-Celsr1-GFP [4]; K14-Cre; Vangl1fl/fl ; Vangl2fl/dTM ;mTmG/+ [28, 29]; and Fz6 KO ; mTmG/+ [30]. K14-Celsr1-GFP-F2A-H2B-RFP transgenic mice were generated by introducing a 2A cleavage site between the coding sequences of Celsr1-GFP and H2B-RFP, and transgenic lines were generated Cancer Institute of New Jersey Genome Editing Facility. Mice were housed in an AAALAC-accredited facility in accordance with the Guide for the Care and Use of Laboratory Animals. All procedures involving animals were approved by Princeton University's Institutional Animal Care and Use Committee (IACUC).

Cell lines

Mouse keratinocytes derived from dorsal epidermis of CD1 mice at P0 (prior to when sex can be externally determined) were used to generate stable lines expressing Celsr1-mRuby3, Celsr1-mNeonGreen, Celsr1-mEos3.2, Celsr1-mTagBFP2, and Celsr1-mTagRFP-T. Each line was generated by cotransfecting the respective pBacK14 vector with pCMV-hyPBase and selecting the cells with G418 starting 24 hr after transfection. Stable cell lines for Celsr1ΔN-mNeonGreen, Celsr1ΔN-mTagRFP-T, and 3xFLAG-Vangl2 were generated via retroviral transduction. Keratinocyte transfections were performed using QIAGEN effectene (Cat. #301427) using an adjusted ratio (8:1 Enhancer, 10:1 Effectene Reagent). Cells were maintained at 37 degrees, 5% CO_2, in E-medium with 50uM calcium [33]. To induce formation of an epithelial monolayer, cells were incubated for 24 hr E-medium with 1.2-1.5mM calcium.

METHOD DETAILS

Molecular cloning and constructs

Constructs used were generated by this study unless otherwise noted: pBacK14-Celsr1-mNeonGreen; pBacK14-Celsr1-mRuby3; pBacK14-Celsr1-mEos3.2; pBacK14-Celsr1-mTagBFP2; pBacK14-Celsr1-mTagRFP-T; K14-Celsr1-ECadCT-GFP; K14retro-Celsr1ΔN-mNeonGreen; K14retro-Celsr1ΔN-mTagRFP-T; K14retro-HA-Celsr1ΔN-GFP; K14-Frizzled6-tdTomato; K14-Fzd6-mCherry [15]; K14-mCherry-Vangl2 [15]; K14retro-3xFLAG-Vangl2. The pBacK14 vector was constructed by flanking the expression cassette of the K14 vector and an added G418 selection cassette with the PiggyBac transposon [31]. Plasmids containing the fluorophores mTagRFP-T, mRuby3, mTagBFP2, and mEos3.2 were gifts from Michael Davidson (Addgene #54586, 74252, 54602, and 54550 respectively). mNeonGreen was a gift from Lynn Enquist. pCMV-hyPBase was obtained from the Wellcome Trust Sanger Institute [31].

Cell mixing assays

Stable cell lines and/or transfected cells with the appropriate constructs were cultured separately before being mixed in approximately 50:50 ratios and replated in high calcium E-medium (1.2-1.5mM). Mixed cell cultures were grown for an additional 16-24 hr to allow time for cell junctions to form. Cells were then either imaged live or fixed with 4% PFA for immunostaining. Dividing cells were identified by the presence of Celsr1-positive puncta or nuclear morphology.

Photoconversion assay

Stable cell lines expressing Celsr1-mTagBFP2 were mixed with those expressing Celsr1-mEos3.2. To avoid photoconversion of mEos3.2 in the entire field of view, dividing cells at the interface between Celsr1-mTagBFP2 and Celsr1-mEos3.2 were identified by mEos3.2 signal alone. Identities of cells were confirmed by imaging the mTagBFP2 channel after the experiment was complete. mEos3.2 was photoconverted using a galvo X-Y miniscanner (Bruker Corporation) equipped with a 405 laser (Coherent) at 10% laser power, 150ms dwell time and an ROI consisting of a single point. For quantification, background signal was subtracted and photobleaching was corrected for using a second photoswitched region in the same field of view.

Celsr1 surface labeling

Keratinocytes were transfected with HA-Celsr1-GFP either alone or with K14-mCherry-Vangl2 or K14-Fz6-mCherry for 36-48 hr and shifted to 1.5mM calcium E-medium for 8-12 hr. To specifically label the surface pool of Celsr1-ΔN, anti-HA antibody was added to media 1:500 on ice for 30 min. Cells were washed 3x in cold PBS, fixed for 10' in 4% PFA and stained with anti-rat 647 antibodies (1:2000) without permeabilization.

Celsr1 recycling assay

Keratinocytes were transfected with HA-Celsr1ΔN-GFP and shifted to 1.5mM calcium E-medium for 8-12 hr. Anti-HA antibody was added to media 1:500 on ice for 30 min. Cells were washed 3x in cold PBS, chased at 37° for 2 hr and fixed for 10' in 4% PFA. Cells were stained with anti-rat 647 antibodies (1:2000) with or without permeabilization to label total and surface HA, respectively, and HA surface levels were quantified as above. For the live imaging experiment, keratinocytes stably expressing HA-Celsr1ΔN-GFP were calcium shifted to 1.5mM calcium E-medium for 8-12 hr and incubated with Alexa Fluor 647-conjugated primary anti-HA antibody for 30-45 min at 1:100 in media at 37°. Cells were washed 3x in warm media and 3x in room temperature PBS. Media was replaced and the cells were imaged immediately. To enrich for mitosis, cells were synchronized with the reversible CDK1 inhibitor RO-3306 (9 μM; Sigma SML0569). Drug was added 8-12 hr prior to the experiment (concomitant with the calcium switch) and was included in all media and incubations except the final washes.

Immunostaining and image acquisition

All samples were fixed with 4% PFA for either 15 min (cells) or 1 hr (tissue). Permeabilization and blocking buffer consisted of PBS/0.1% Triton X-100/5% NDS for cells and PBS/0.3% Triton X-100/5% NDS for tissues. Samples were blocked for a minimum of 2 hr and incubated with primary antibody in blocking buffer overnight at 4°C. Secondary was conducted in blocking buffer for 3 hr at RT or 4°C overnight. Antibodies used in this study: guinea pig-anti-Celsr1 at 1:1000 [15], goat-anti-Fzd6 at 1:200 (R&D #AF1526), rat-anti-Vangl2 at 1:1000 or 1:200 (clone 2G4; gift from Jean-Paul Borg [27]; Millipore #MABN750), rat-anti-E-Cadherin at 1:1000 (clone DECMA-1; Thermo-Pierce #MA1-25160), rabbit-anti-Rab7 at 1:200 (Cell Signaling #D95F2), mouse-anti-FLAG at 1:1000 (Sigma #F1804), rat-anti-HA at 1:500 (Roche #11867423001), 647-mouse-anti-HA at 1:100 (Cell Signaling #3444). Nuclei were labeled with Hoechst. Some fixed samples and all live imaging was performed using a Nikon spinning disc confocal system equipped with a Yokogawa CSU-21 and a Hammamatsu ORCA-Flash4.0 sCMOS camera. Remaining images of fixed samples were acquired on an inverted Nikon A1 or A1R-Si confocal microscope, on a Nikon Eclipse Ti stand (Nikon Instruments) equipped with a GaASP detector.

QUANTIFICATION AND STATISTICAL ANALYSIS

Quantification of vesicle enrichment

The anterior-posterior (AP) axis of the skin at E15.5 was determined using hair follicle orientation. Z stacks were collected of individual cells at the specified stages of mitosis (determined by nuclear morphology). Cells were manually bisected perpendicular to the angle of the AP axis. The Pearson's correlation (*r*) was calculated for the overlap between Celsr1 and either Vangl2, Fzd6, or E-Cadherin in both the anterior and posterior halves of cells for the entire Z stack using the "Colocalization Test" function in Fiji. Data was represented as a ratio of the calculated *r* for anterior or posterior halves to the calculated *r* for the whole cell.

Quantification of Celsr1 surface labeling

To quantify HA-Celsr1-GFP surface levels, maximum intensity projections were hand segmented, and the background subtracted, mean fluorescent intensity of HA and GFP signals were calculated for each cell. Data was represented as the ratio of surface HA to GFP intensity per cell.

Quantification of Vangl2 asymmetry

Vangl2 asymmetry were calculated with Packing Analyzer V2 software as described [32]. Basal cell boundaries were segmented based on membrane-tdTomato label. The axis and magnitude of polarity was based on the perimeter intensity of Vangl2, normalized per image by the corresponding average cell boundary Vangl2 intensity. Data were plotted on a circular histogram using the polar plot function in MATLAB, and histograms were weighted by the average magnitude of polarity within each bin. The magnitude ; (M_P) and orientation of average Vangl2 polarity were overlaid as a line on top of the circular histogram in which the length of the line reflects the magnitude and the orientation of the line refers to the axis of average Vangl2 polarity ([26].

Statistical Analysis

The statistical details of experiments can be found in the figure legends, including the statistical tests used, exact value of n, what n represents, definition of center and dispersion measures (e.g., mean, SD, SEM). For box and whisker plots, center is the mean, boxes represent 25-75 percentiles, whiskers represent min to max. Significance was defined by the p value *$p < 0.05$, **$p < 0.01$, ***$p < 0.001$, ****$p < 0.0001$. An F test was used to compare variances between samples.